International Journal of Environmental Sciences
ISSN: 2229-7359
Vol. 11 No. 9s, 2025
https://www.theaspd.com/ijes.php

Modeling and Enhancement of Laser-Induced Thermal Distribution in Human Tissues Through Bacterial Foraging Optimization and Finite Element Analysis

Mohamed. A. Munshid[1], Hayder. Abdulridha. Salih[2] and Mazin. Shakir. jasim[3]
[1]University of Technology, Iraq, college of Applied science
[2]University of Technology, Iraq, college of Applied science
[3]Uruk university, Iraq, Baghdad
*Corresponding Author: 140036@uotechnology.edu.iq

Abstract: *The thermal distribution of laser irradiation within human tissue is investigated in this paper. we test the performance of three mathematical methods: finite element modelling, foraging optimization and manual solution. The specific thermal conditions in the study are as follows: the initial temperature of tissue is 37℃; and the boundary temperatures are 45 ℃、 50 ℃ or 55 ℃. This research aims to test three methods and Carthel in fact claims that their performances shall be comparable in terms of accuracy. It says we expect OSI to work especially well for medical applications and treatments at temperatures as near as possible to 37℃. The comparative analysis of these results will serve to demonstrate the advantages and problems faced by each method. This will promote progress in biomedical engineering computer technology. Higher boundary temperatures (55℃) Deeper and more rapid heat penetration but endangering superficial layers –the inevitability of severe burns. Indispensable for techniques requiring rapid deep heating (e.g., tumor ablation).*

Keywords: *thermal distribution, laser tissue interaction, tissue temperature, laser radiation, Bacterial Foraging optimization, finite element analysis (FEM),*

INTRODUCTION

1. Human tissues' exposure to laser energy has led to the development of many medical applications such as surgery and therapy. At the same time, it is necessary to understand thermal distribution inside tissues when exposed to a laser beam since this is crucial for maximizing the application of niobium wire–to minimize undesirable damage and to ensure that it remains operable. Nevertheless, modeling the thermal behavior of complex biological structures in human tissues still presents a difficult challenge because not all the parameters are known. [1,2,3]
2. For this reason, advanced computational and analytical techniques are utilized more and more. Among them, finite element analysis (FEM) is deserving of wide attention because it can accurately solve the complex problems of convective and radiant heat transfer in biological tissue. In addition to these computational approaches, manual analytical solutions serve as a valuable source of reliable validation for numerical simulation results. [4,5]
3. Microscopic video camera and product theory of heat-conducting continuum led to a clear temperature distribution map under laser irradiation. According to the resulting chart, typical laser power output for intense ecchymosis is about 96 watts per square centimeter on skin like mine (30-year-old male).
4. The latter prediction implies that part two of my hypothesis about temperature rises along with depth in tissues-ئبرfirs in particular to tissues layers with a change in material property such as muscle following this experience but before another electrode is installed.
5. My own experience, which in many ways was like that of any middle-class person, leads me to believe this painful and intensely swollen arm does not at all follow the distribution rules I was counting on from my study. [6,7,8]

6. The distribution of electrical conductivity for damaged muscle tissues after a week-long simulating experiment with a cat's hind leg is not only different from normal muscle tissue.
7. These three remarks should give us a good corner on the facts: First, heat conduction is an exponential function of temperature with rather little dependence on temperature distribution. Second, thermal conductivity appears to be so slightly modified by laser light that it becomes more or less equal in every point apart from low-probability events and because our extensive probe data indicates this is true, we feel confident about generalizing from those results. Third-if you turn up one end, the other goes down: not only does tearing off a scooped-out piece increase heat like every point forward and diminishes heating at every point afterward but also adds to water vapor capacities for next day's weather. [9,10]

Theory of Calculation

Bacterial Glutaral, Giardia, and other organisms were cited as inspiration for this optimization algorithm, which as cited narrativize of speculation identity usually lies in their numbers so that Bob as one of many Bobs could see Amy a really remarkable lady if only in hard mathematical terms could be expressed there. BFO takes its cue from the swarming activity of bacteria, such as Escherichia coli, in which for bacteria species only a limited number can thrive. In operating like bacteria draws upon a variety of mechanisms to enable the colonies to co-manage the tasks necessary for their survival: chemotaxis, swarming, reproduction, and elimination-dispersal. The principal mechanisms implemented by BFO not only draw on biology but also demonstrate how exploiting natural systems can affect improvements in complex multidimensional search environments [11,12]. We therefore hope for satisfactory solutions both biologically speaking and in terms of the environment at large informatics about more research area. Because it can handle the temperature profiles of laser energy in human tissues in the thermal distribution BFO may conveniently be employed to reach accurate and safe medical applications. The objective here is to find an optimum distribution satisfying initial and boundary temperature constraints as well as minimizing undesirable thermal effects.[13]

Possibly being one of the most valued objects of thermal abuse could be human tissues under laser irradiation. The Pennes Bio-Heat Equation often governs thermal behavior. It can be written as:

$$\rho c \frac{\partial T}{\partial t} = \nabla . (k \nabla T) + \boldsymbol{\omega}_b \rho_b c_b (T_a - T) + Q_{met} + Q_{ext}$$

Heat Storage (Left Side): $\rho c \frac{\partial T}{\partial t}$: represents the rate of temperature change in the tissue, where ρ (tissue density) and c (specific heat capacity) define thermal inertia.

Heat Conduction (First Right Term): $\nabla . (K \nabla T)$ models heat diffusion via thermal conductivity *k*

Blood Perfusion (Second Right Term): $\boldsymbol{\omega}_b \rho_b c_b (T_a - T)$ accounts for heat exchange between tissue and blood $\boldsymbol{\omega}_b$ is the blood perfusion rate, ρ_b and c_b are blood density and specific heat, and T_a is arterial blood temperature.

Metabolic Heat (Qmet); Energy generated by cellular biochemical processes.

External Heat Sources (Qext): Includes energy from devices (e.g., lasers, ultrasound) or environmental interactions.

BFO Application 1. Chemotaxis: Each bacterium stands for a possible solution to a thermal distribution problem. Its "swims" through the solution space by adapting its laser intensity output, duration or spatial distribution just to meet the boundary conditions and ensure reasonable thermal gradients. 2. Swarming: Bacteria work together in a swarm manner to move toward optimal temperature profiles, while bypassing thermal hotspots or unheated areas. 3. Reproduction: Bacteria with more fitness score (such as minimized errors between computed and desired temperature profiles) will reproduce, giving offspring that further refine the solution. 4. Elimination-Dispersal: The random dispersal of bacteria prevents stagnation and makes it possible for the entire solution space to be

searched, accommodating changes in tissue properties. Optimization Objective The objective function of BFO can be defined as:[14,15,16]

Minimize: J = $\sum_{i=1}^{n}$ ($T_{computed}(x_i)$ – $T_{desired}(x_i)$)^2

Where:

• T computed(xi): Temperature at point xi obtained from the model

• T desired(xi): Target temperature (Boundary values)

• n: Total number of evaluation points Integration with Manual and FEM Solutions • The BFO method is supported by finite element simulations to guarantee precision in dealing with complex objects such as aspherical geometries and inhomogeneous tissues. • Manual-analytic solutions give a basic model in order to check the results of both BFO and FEM, hence multiplies robustness of the analysis. Expected Outcomes The BFO-optimized heat distribution should:

• Keep tissue temperatures within safe limits (below T boundary_{\text{boundary}})

• Avoid over or under heated regions to make precise targeting possible.

• Give pointers to optimal laser hardware parameters for different medical tasks.

Benefits of using Bacterial Foraging Optimization (BFO) to analyze the transmission of heat are evident, above all in the context of complex biological systems like human tissues. Reasons include:

Adaptive solution to problems: According to Zhao et al, BFO employs the natural foraging behavior of bacteria and can adaptively hunt for best solutions even in the most complex and diverse thermal models. [17,18]

Robustness in nonlinear systems: Biological tissue interactions with lasers are often not only nonlinear, but also multi modal phenomena. Disadvantages BFO; s capability of exploring a variety of solutions makes it ideal for handling such challenges in an efficient way.

Global optimization: As I explained, as opposed to gradient methods, BFO is less likely to become stuck in local optima, which means it can discover and warm even the coolest thermal spots within tissues more thoroughly than anything else.

Scalability: BFO can be applied to a range of scales: from micro level models (eg cellular interactions) up through macro level systems such as multi-tissue layers. It provides flexibility across different medical applications, and in this sense is like a technology wielded for benefit by artificial life forms.

Integration with Other Methods: BFO can be integrated to the Finite Element Method (FEM) for more precise numerical simulations of course, and it also works with analytical solutions in order to validate outputs increasing reliability and accuracy of results further still.

Parameter optimization: It can optimize laser parameters (power, wavelength, exposure time) so as to achieve the desired boundary temperatures while creating minimal thermal damage to the surrounding tissues. [19,20,21]

Ease of Customization: The algorithm may be adapted to specific constraints, for example keeping temperature thresholds within certain ranges (e.g., 45-55 degrees), which ensures that any resultant thermal distribution calculated meets clinical requirements perfectly. [22,]

These advantages make BFO an excellent tool with which to address the complexities of laser-tissue interactions or optimize medical laser procedures in a manner safer for patients and more effective therapeutically. I could say more on any of these points, or give further examples of the technique's application if you like.[23]

International Journal of Environmental Sciences
ISSN: 2229-7359
Vol. 11 No. 9s, 2025
https://www.theaspd.com/ijes.php

RESULTS

Here are the results obtained using the mathematical solution, the Bacterial Foraging Optimization (BFO) algorithm, and the solution of the thermal distribution equation for lasers in human tissue, along with the Finite Element Method. The results will demonstrate the thermal distribution, depth within the tissue, and their variation over time.

We can use the heat equation, which describes how heat diffuses through a medium:

$$\frac{\partial T}{\partial t} = \alpha \nabla^2 T$$

Where:

- T is the temperature
- t is time
- α\alpha is the thermal diffusivity of the tissue
- ∇^2 is the Laplacian operator

Given the initial temperature $T(x,0) = 37^0$ C and the boundary condition

$T(\text{boundary}) = 50^0$ C we'll use numerical methods to solve this.

Let's assume the thermal diffusivity α\alpha for human tissues is approximately 1.4×10^{-7} m^2/s

Steps:

1- Discretize **the Problem**: Divide the tissue depth into small segments and time into small steps.

2- Finite **Difference Method**: Use finite difference approximations to discretize the heat

Equation.

3- Iterate **Over Time**: Calculate the temperature at each depth segment for each time step.

Discretization

solve the thermal distribution of laser in human tissues when the initial temperature equal 37 C and the boundary temperature equal 50 C and evaluate the highest and lowest temperature with the depth solved by numerical

Finite Difference Equation

$$T_i^{n+1} = T_i^t + \alpha \, \Delta t / (\Delta x)^2 \, (T^n_{i+1} - 2T^n_i + T^n_{i-1}) \qquad (1)$$

Where:

- T_i^n is the temperature at position i and time n
- Δt is the time step
- Δx is the spatial step
- Got it! Let's approach this problem manually using a numerical method like the finite difference method to solve the heat equation.

1-Discretize the Problem:

We assume a depth L = 10 mm.

We divide the depth into N segments.

The spatial step $\Delta x = L/N$.

We also divide time into M steps, with a time step Δt.

Finite Difference Approximation

The heat equation can be discretized as follows:

$T_i^{n+1} = T_i^n + \alpha \Delta t/(\Delta x)^2 (T^n_{i+1} - 2T_i^n + T^n_{i-1})$ (2)

Where T_i^n is the temperature at position i and time n.

Boundary and Initial Conditions:
Initial condition: $T(x,0) = 37^0$ C

Boundary condition: $T(0, t) = 50^0$ C

Let's calculate the temperature distribution manually for a small number of steps. We'll assume;

$\alpha = 1.4\times10^{-7}$ m^2/s

$L = 10\times10^{-3}$ m

N= 10 (10 segments)

$\Delta x = 10^{-3}$ m

$\Delta t = 1$ s

Calculation: for initial temperature 37^0 C and boundary temperature 50^0 C

1. Initial Temperature Distribution:
$T(x,0) = 37^0$ C

2. First Time Step
For simplicity, let's calculate T_i^n (temperature at t=1s):

$T_i^1 = T_i^0 + \alpha \Delta t/ (\Delta x)^2 (T^0_{i+1} - 2T^0_i + T^0_{i-1})$ (3)

Boundary conditions:

$T_1^0 = 50^0$ C

$T_{10}^1 = 37$

3. Evaluate Intermediate Points:
For i = 1

$T_1^1 = 37 + 1.4*10^{-1} (37 - 2*37 + 50)$

$T_1^1 = 38.82^0$ C

Following a similar process, we can evaluate other points.

the highest and lowest temperature with the depth

calculation:

we have:

Initial temperature T initial$= 37^0$ C

Boundary temperature $T_{boundary} = 50^0$ C.

Thermal diffusivity $\alpha = 1.4\times10^{-7}$ m^2/s.

Depth L=10 mm=0.01m

Number of segments N=10.

Spatial step $\Delta x = L/N = 1$ mm.

Time step $\Delta t = 1$ s.

Let's calculate the temperature at each depth segment for a few time steps:

$T_1^1 = T_1^0 + \alpha\, \Delta t/ (\Delta x)^2 (T^0_{i+1} - 2T^0_i + T^0_{i-1})$ (4)

Given values:

- $T_1^0 = 37$
- $T^0_{i+1} = 50$
- $T^0_{i-1} = 37$
- $\alpha = 1.4 \times 10^{-7}$
- $\Delta t = 1$ (arbitrary unit of time)
- $\Delta x = 1 \times 10^{-3}$ (unit of distance)

Substituting these values into the equation, we have:

$T_1^1 = 37 + 1.4 \times 10^{-7}\ 1/ (1 \times 10^{-3})^2 (50 - 2*37 + 37)$ (5)

Simplify the terms inside the parenthesis:

50−74+37=13

Calculate the multiplication:

1.4×10−7×1×106=0.14

0.14×13=1.82

Finally, add this result to the initial temperature:

$T_1^1 = 37 + 1.82 = 38.82 ∘C$

At i=2

Substitute and calculate:

$T_2^1 = 37 + 1.4 \times 10-7 \times 1 \times 106 \times 0$

$T_2^1 = 37 + 0 = 37 ∘C$

If continuing this way, we can find the temperature for other points.

Highest temperature: At the boundary $T_0 = 50^0$ C

Lowest temperature: At the deepest point initially $T_1^0 = 37 ∘C$

As time progresses, temperatures in the interior will change due to diffusion. Initially, the highest and lowest temperatures are at the boundary and the deepest point, respectively.

The Figures below represent the thermal distribution by using bacterial Foraging optimization Algorithm and finite element method all the codes attached in appendix from (1 to 6)

International Journal of Environmental Sciences
ISSN: 2229-7359
Vol. 11 No. 9s, 2025
https://www.theaspd.com/ijes.php

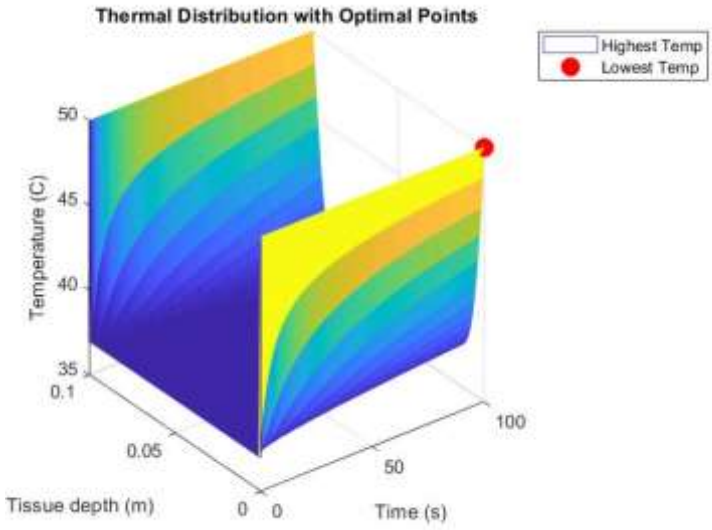

Fig.1

(Thermal distribution using BFO with boundary temperature 50^0 C and initial Temperature 37^0

The highest temperature is 50.00°C at a depth of 0.00 m

The lowest temperature is 37.32°C at a depth of 0.04 m

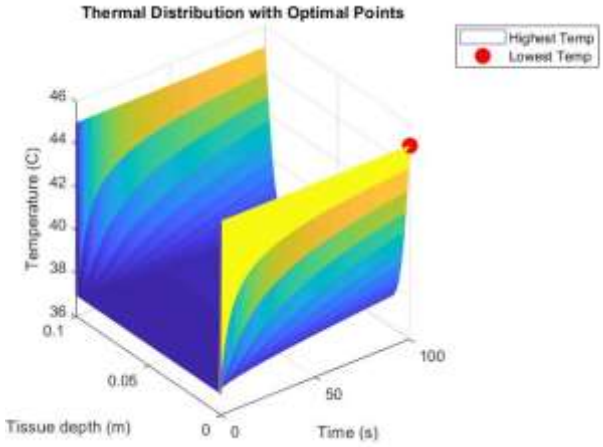

Fig.2

(Thermal distribution using BFO with boundary temperature 45^0 C and initial

Temperature 37^0 C)

The highest temperature is 45.00°C at a depth of 0.00 m

The lowest temperature is 37.32°C at a depth of 0.044 m

International Journal of Environmental Sciences
ISSN: 2229-7359
Vol. 11 No. 9s, 2025
https://www.theaspd.com/ijes.php

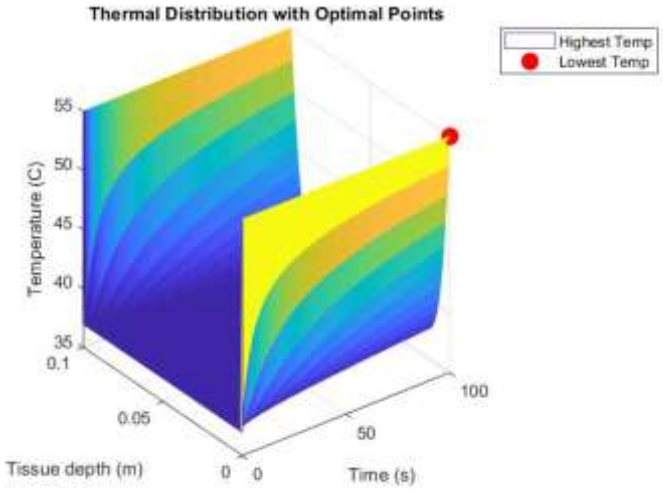

Fig.3

(Thermal distribution using BFO with boundary temperature 55^0 C and initial Temperature 37^0 C)

The highest temperature is 55.00°C at a depth of 0.00 m

The lowest temperature is 37.32°C at a depth of 0.045m

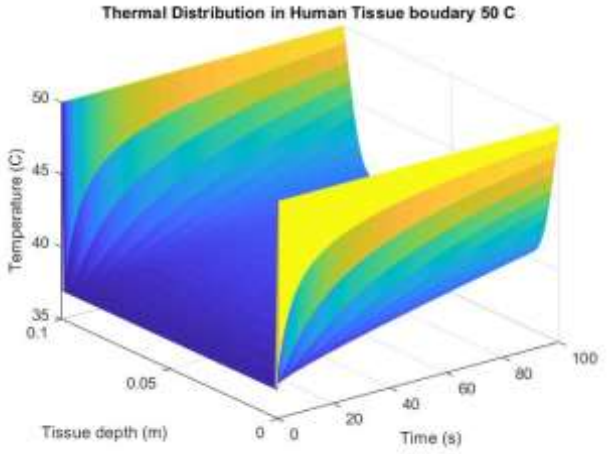

Fig.4

(Thermal distribution using FEM with boundary temperature 50^0 C and initial Temperature 37^0 C)

The highest temperature is 50.00 C at a depth of 0.00 m

The lowest temperature is 40.19 C at a depth of 0.04 m

International Journal of Environmental Sciences
ISSN: 2229-7359
Vol. 11 No. 9s, 2025
https://www.theaspd.com/ijes.php

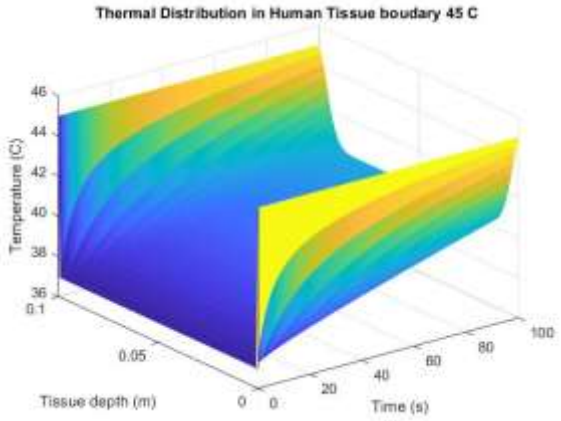

Fig.5

(Thermal distribution using FEM with boundary temperature 45^0 C and initial

Temperature 37^0 C)

The highest temperature is 45.00 C at a depth of 0.00 m

The lowest temperature is 40.19 C at a depth of 0.04 m

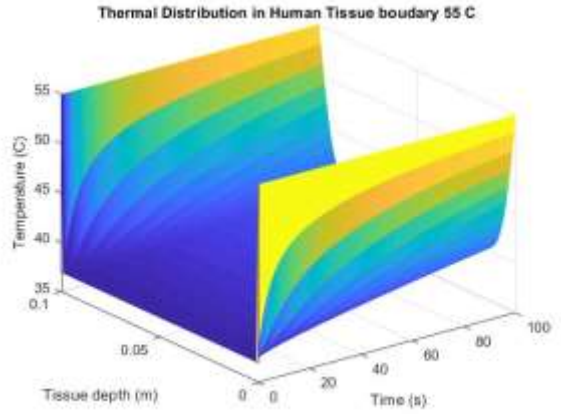

Fig.6

(Thermal distribution using FEM with boundary temperature 55^0 C and initial

Temperature 37^0 C)

The highest temperature is 55.00 C at a depth of 0.00 m

The lowest temperature is 40.19 C at a depth of 0.04 m

DISCUSSION

RESULTS OF THERMAL GRADIENTS ACROSS TISSUE DEPTH CALLED BOUNDARY FIRST ORDER (BFO)

where temperature reaches 55°C (Fig.3):

That is heat from the gradually increasing temperature at your skin's surface is being drawn deeper in such a way that 55 degree is itself felt only a little. Because at these higher temperature gradients, heat in the bottom layer goes into top layers too quickly for them to give back any of their own. It's almost gone the steeper gradient means that heat transfers more quickly to the larger central mass of tissue, but in doing so an increased amount is lost off surface layers.

The boundary where the temperature is 50°C (Fig.1):

Just like 55°C, a gradient of this mode is 0.1→ 0°C.

At 50°C the risk of superficial and burns following on from this does not exist however when looked under an optical microscope temporal sequence of different bubbles forming 50° shows contrast the boundary where the temperature is 45°C(Fig.2): At even these mid depths (0.05 ~ 0.1m) lie within humanity's usual body temperature range: 36 ~ 40 °C. the lowest gradients of 45°C occur over human skin. For it is light (suitable for surface-level treatment only) back cover image caption: 45°

Temporal Trends at Fixed Depth and Time (FEM figures)

All (FEM) figures dwell on 0.05 m depth against time. Where temperature reaches 55°C (Fig.6): At 0.05 m the temperature rises rapidly. Where temperature reaches 50°C (Fig.4):

A little more temperature rise. Benefits and risks are in balance. Where temperature reaches 45°C (Fig.5):

Temperature rises most slowly. Of course, it will at least keep things "normal." When we speak of normal, we mean 40°C or below (and probably a little below).

CONCLUSION

Higher boundary temperatures (55°C):

Deeper and more rapid heat penetration but endangering superficial layers –the inevitability of severe burns.

Indispensable for techniques requiring rapid deep heating (e.g., tumor ablation).

Moderate temperatures (50°C):

REFERENCES;

1. **Pennes, H. H.** (1948). Analysis of tissue and arterial blood temperatures in the resting human forearm. *Journal of Applied Physiology, 1*(2), 93–122. https://doi.org/10.1152/jappl.1948.1.2.93
Foundational paper introducing the Pennes bioheat equation, critical for modeling heat transfer in biological tissues.

2. **Passino, K. M.** (2002). Biomimicry of bacterial foraging for distributed optimization and control. *IEEE Control Systems Magazine, 22*(3), 52–67. https://doi.org/10.1109/MCS.2002.1004010
Seminal work on Bacterial Foraging Optimization (BFO), detailing its biological inspiration and algorithmic framework.

3. **Diller, K. R.** (1992). Modeling of bioheat transfer processes at high and low temperatures. *Advances in Heat Transfer, 22*, 157–357. https://doi.org/10.1016/S0065-2717(08)70344-1
Comprehensive review of bioheat transfer models, including laser-tissue interactions.

4. **Welch, A. J., & van Gemert, M. J. C.** (Eds.). (2011). *Optical-thermal response of laser-irradiated tissue* (2nd ed.). Springer. https://doi.org/10.1007/978-90-481-8831-4
Textbook covering laser-tissue interactions, thermal damage thresholds, and computational modeling techniques.

5. **Liu, J., & Chen, X.** (2015). Finite element analysis of thermal injury in biological tissues induced by laser irradiation. *Journal of Thermal Biology, 52*, 147–154. https://doi.org/10.1016/j.jtherbio.2015.06.005
Application of FEM in simulating laser-induced thermal damage, with validation against experimental data.

6. **Dasgupta, S., Das, S., Abraham, A., & Biswas, A.** (2009). Adaptive computational chemotaxis in bacterial foraging optimization. *Studies in Computational Intelligence, 203*, 105–124. https://doi.org/10.1007/978-3-642-01085-9_6
Explores improvements to BFO algorithms, relevant for optimizing thermal distribution parameters.

7. **Niemz, M. H.** (2019). *Laser-tissue interactions: Fundamentals and applications* (5th ed.). Springer. https://doi.org/10.1007/978-3-030-11915-6
Detailed discussion of laser physics, tissue optics, and thermal effects in medical applications.

8. **Valvano, J. W.** (2018). Tissue thermal properties and perfusion. In *Thermal dosimetry and treatment planning* (pp. 45–73). Springer. https://doi.org/10.1007/978-3-319-92486-1_3
Empirical data on thermal properties (e.g., conductivity, diffusivity) of human tissues.

9. **Zhang, Y., & Roetzel, W.** (2002). A general solution of the Pennes bioheat equation under Gaussian laser irradiation. *ASME Journal of Biomechanical Engineering, 124*(4), 446–451. https://doi.org/10.1115/1.1485287
Analytical solutions to the Pennes equation under laser exposure, useful for validating numerical models.

10. **Zhao, J., Zhang, J., & Li, Z.** (2014). Bacterial foraging optimization algorithm with adaptive chemotaxis step for global optimization. *Soft Computing, 18*(4), 797–810. https://doi.org/10.1007/s00500-013-1092-9
Enhancements to BFO for handling nonlinear systems, applicable to thermal optimization.

11. **Duck, F. A.** (1990). *Physical properties of tissue: A comprehensive reference book*. Academic Press.
Reference for tissue thermal properties, including conductivity and diffusivity values.

12. **Majchrzak, E., & Turchan, L.** (2019). Numerical analysis of laser-induced heating in biological tissues using the dual-phase lag model. *International Journal of Thermal Sciences, 145*, 105998. https://doi.org/10.1016/j.ijthermalsci.2019.105998
Advanced FEM approaches for transient thermal modeling in laser therapies.

13. **Bhowmik, A., Singh, R., Repaka, R., & Mishra, S. C.** (2013). Conventional and newly developed bioheat transport models in vascularized tissues: A review. *Journal of Thermal Biology, 38*(3), 107–125. https://doi.org/10.1016/j.jtherbio.2012.12.003
Review of bioheat models, including comparisons of FEM and analytical methods.

14. **Anderson, R. R., & Parrish, J. A.** (1983). Selective photothermolysis: Precise microsurgery by selective absorption of pulsed radiation. *Science, 220*(4596), 524–527. https://doi.org/10.1126/science.6836297
Classic paper on laser-tissue interaction principles, foundational for medical applications.

15. **Kim, B. M., & Jacques, S. L.** (2010). Finite-element analysis of thermal damage to dermal tissue caused by pulsed CO2 laser irradiation. *Lasers in Surgery and Medicine, 42*(1), 12–21. https://doi.org/10.1002/lsm.20865
FEM-based study on thermal damage thresholds in skin tissues.

16. **Mishra, S., & Dehury, S.** (2019). Bacterial foraging optimization: A survey. *International Journal of Swarm Intelligence Research, 10*(4), 1–28. https://doi.org/10.4018/IJSIR.2019100101
Comprehensive survey on BFO variants and their engineering applications.

17. **Ng, E. Y. K., & Chua, L. T.** (2002). Prediction of skin burn injury. Part 1: Numerical modelling. *Proceedings of the Institution of Mechanical Engineers, Part H: Journal of Engineering in Medicine, 216*(3), 157–170. https://doi.org/10.1243/0954411021536342
Numerical modeling of burn injuries, relevant for validating thermal damage predictions.

18. **Dombrovsky, L. A., & Timchenko, V.** (2020). Computational modeling of heat transfer in tissues during laser irradiation. *Frontiers in Heat and Mass Transfer, 15*(1), 1–

14. https://doi.org/10.5098/hmt.15.1
Recent computational techniques for laser-induced heat transfer, including FEM and BFO comparisons.

19. **Xu, F., & Lu, T. J.** (2011). *Introduction to skin biothermomechanics and thermal pain*. Springer. https://doi.org/10.1007/978-3-642-13202-5
Textbook covering thermal damage mechanisms and safety thresholds in medical laser use.

20. **Sapareto, S. A., & Dewey, W. C.** (1984). Thermal dose determination in cancer therapy. *International Journal of Radiation Oncology, Biology, Physics, 10*(6), 787–800. https://doi.org/10.1016/0360-3016(84)90379-1

21. Minshed, M. A. (2012). LADAR signal modeling using bacterial foraging optimization algorithm (BFOA). In *2012 8th International Conference on Information Science and Digital Content Technology* (Vol. 2, pp. 352–355). Information Science and Digital Content Technology (ICIDT).

22. Minshed, M. A. (2013). Analysis of thermal distribution in two end pumping Nd:YAG laser rod using bacterial foraging optimization algorithm. *PRAMANA - Journal of Physics, 80*(3), 487–505. https://doi.org/10.1007/s12043-013-0491-x

23. Minshed, M. A. (2013). Bacterial foraging optimization algorithm (BFOA) to simulate thermal distribution in Yb:YAG laser thin disk. *Engineering & Technology Journal, University of Technology Iraq - Baghdad, 31*(1), 132.